

Investigation of acoustic properties of various
wood varieties through vibrational analysis

Rio Weil & Annika MacKenzie

August 13, 2019

Abstract

Vibrational analysis was carried out on 6 different species of wood, *Quercus alba*, *Acer macrophyllum*, *Pinus monticola*, *Pseudotsuga menziesii*, *Thuja plicata*, and *Picea engelmanni*. Resonant frequencies of the (1,1) and (2,0) modes of vibration were analyzed with Audacity, and modulus of elasticity was determined via beam approximation. Quality factor of oscillations of the (2,0) mode and Acoustic Conversion Efficiency of each specimen were determined. Out of the tested specimens, *Pseudotsuga menziesii* was found to have the highest Acoustic Conversion Efficiency, possibly due to having the most consistent wood grain. A new unified model was derived to approximate resonant frequencies of the (2,0) mode for rectangular plates by combining past models for square plates and bars.

Contents

1	Introduction	2
2	Methods	3
3	Introduction of applied formulae	5
3.1	Elastic moduli and acoustic conversion efficiency	5
3.2	Modelling resonant frequencies	6
4	Discussion of results	8
4.1	Frequency and frequency modelling	8
4.2	Young's modulus and acoustic conversion efficiency	11
5	Discussion of errors	14
6	Conclusion	16
7	Acknowledgements	17
8	Appendix - Supplemental graphs	18
9	References	23

1 Introduction

When selecting wood for instrument construction, specific species have traditionally been favoured. In violin soundboards, generally only 3 species of *Picea* genus woods are used [1], due to their superior sound transmission. The important physical characteristics that determine this are the Young's modulus of Elasticity and Internal Friction.

Young's modulus is a mechanical property of material that is defined as the ratio of stress and strain along an axis. It can be measured via mechanical tensile or bending testing, or determined through vibrational analysis.

Internal friction describes the friction between particles as the wave propagates through the material. It can be determined through the "Quality Factor", which describes the energy loss (dampening) of a material while it oscillates. A higher value indicates lower energy loss.

When combined with specific gravity, a value calculated by dividing wood density by the density of water, an index known as Acoustic Conversion Efficiency (ACE) can be calculated. This ratio indicates the ability of a material to convert the energy provided to it into vibrations, creating sound. High values indicate effective sound conversion, and indicates suitability of a species of wood for use in soundboards [1].

These values vary widely among species and have been found in large part to be determined by the cell walls of a type of wood, in specific the microfibril angle of the cell walls [1]. This is the angle between the microfibrils of the secondary cell wall and the long axis of the cell, and it correlates strongly with overall stiffness of the wood [2]. The straightness of the grain also determines which vibration modes dominate, and thus the efficiency of the vibration.

To calculate many of these values the resonant frequency of different vibrational modes are measured. In this experiment, a free-free system, which allows the edges of the plate to oscillate, was studied with regard to rectangular wooden plates.

However, when looking at the vibration of wooden rectangular plates in a free-free system an interesting problem arises. The differential equation that describes the oscillations of a wooden rectangular plate requires boundary conditions in order to solve for the specific coefficients of the system. In the case of supported or clamped edges, the sides are held and so the boundary condition for all modes is the lack of movement at the edges. However, for free-free systems the entire system is allowed to vibrate freely. Nodal areas do exist, however they change location for each mode. Thus, there are no constant boundary conditions which the equation can be solved with. Instead, complex numerical approximations (Rayleigh Ritz Equation), or approximations based on similar shapes such as square plates or bars (for which solutions exist) can be used [3].

The aim of this experiment was to use frequency analysis to determine which of the tested species was most suitable for soundboard use, as well as to find a simple model to predict the frequency of the samples.

2 Methods

A dried sample of each of the tested wood species was cut into 10 pieces of dimensions of 15 cm by 9 cm by 1.9 cm. The tested species of wood were *Quercus alba* (White oak), *Acer macrophyllum* (Bigleaf maple), *Pinus monticola* (Western white pine), *Pseudotsuga menziesii* (Douglas fir), *Thuja plicata* (Western red cedar), and *Picea engelmannii* (Engelmann spruce). Notable, samples of all wood types excepting that of *Pseudotsuga menziesii* had inconsistencies in wood grain to varying degrees. Measurements of length, width, thickness and mass of each piece were taken with a Mastercraft caliper and an O’Haus balance. Values were averaged from 5 repeated measurements.

Preliminary frequency analysis of each wood piece was conducted using the waterfall function of iSpectrum software. The sample was held at a node of the target moded while the sample was tapped along its length and width. iSpectrum’s Fast Fourier Transform (FFT) algorithm converted input audio into a frequency graph with sound intensity of particular frequency shown by density of coloured pixels. With continuous tapping, bands of pixels were created at the resonant frequencies. By taking note of where certain frequency bands disappeared, the nodal lines and corresponding vibrational modes could be identified. The modes identified for the majority of the pieces were the (1,1) torsional mode, which has one nodal line in each axis, and the (2,0) longitudinal mode [4], which has two nodal lines perpendicular to the length.

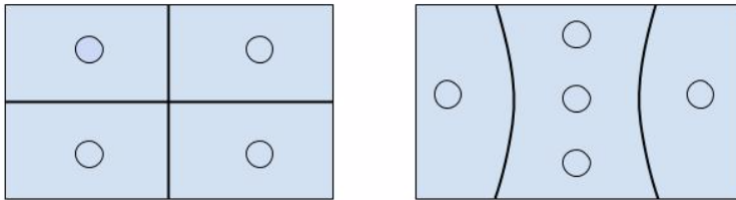


Figure 1: *Measured vibrational modes of the wood samples. (1,1) mode pictured on left, (2,0) mode pictured on right. Lines represent nodes, and circled represent areas of high oscillation tapped for the frequency measurements.*

Once the approximate frequency of a mode was identified, the exact frequency measurement was performed using Audacity. The wood sample was held at the node and tapped in several areas, as demonstrated in Figure 1 above. The sound was recorded with a studio-quality microphone with flat frequency response, at a sample rate of 44100 kHz. Using Audacity’s FFT algorithm, an intensity vs. frequency plot was created for each tap and the peak closest to the approximated frequency was found and recorded. A sample frequency plot is shown in Figure 2 below. 20 taps were analyzed, and the average of the recorded frequencies was taken as the resonant frequency for that mode of vibration. This was repeated for each sample, and the mean of the 10 samples

was taken as the resonant frequency for that species of wood.

Bandwidth Δf of the (2,0) resonant frequency peaks were determined by measuring the width of the resonant peak 3dB below the maximum via pixel counting, where one pixel corresponded to 16.7Hz of width on the display used. Measurements of bandwidth were averaged from 10 taps per sample.

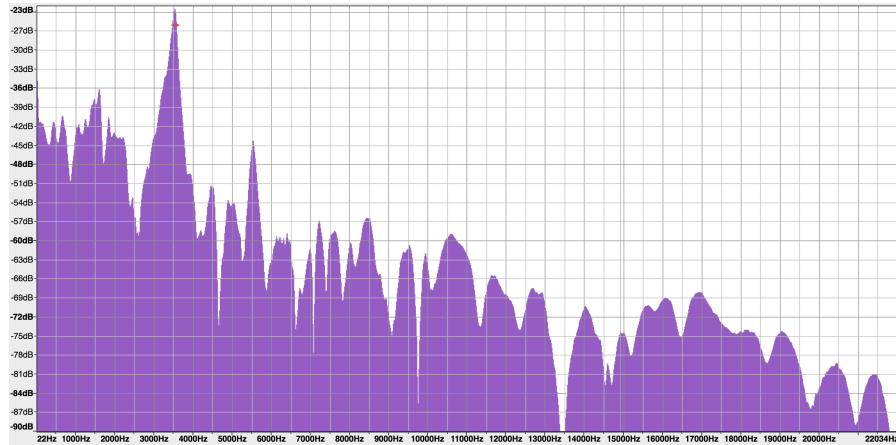


Figure 2: *Sample Audacity frequency spectrum plot of one tap on /textitPinus monticola. The resonant frequency here can be determined to be 3543 Hz.*

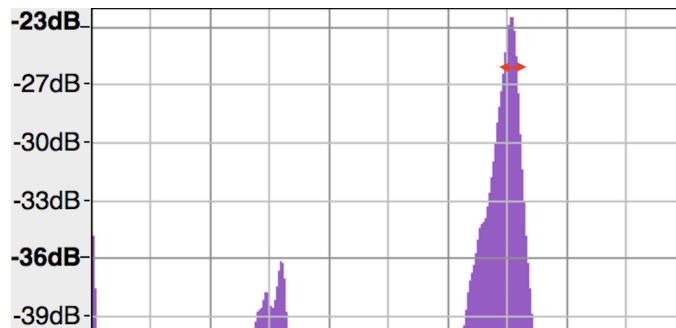


Figure 3: *Peak zoom of the frequency plot in Figure 3. By counting the pixels of the width of the peak 3dB from the maximum, the bandwidth Δf can be determined.*

Standard error propagation methods were used to determine error in calculated values.

3 Introduction of applied formulae

3.1 Elastic moduli and acoustic conversion efficiency

In their 2016 paper, Hamdam et al. [5] used the following equation to determine the Young's modulus of a vibrating free-free rectangular beam:

$$E_d = \frac{4\pi^2 f_0^2 L_x^4 A p}{I m_n^4}. \quad (1)$$

Here, f_0 is the resonant frequency of the mode, L_x is the beam length, A is the cross-sectional area of the beam, p is the beam density, m_n is a constant associated with modal number, where $m_1 = 4.7300$ [6], and I is the second moment of area of a rectangle of width L_y and thickness h .

$$I = \frac{L_y h^3}{12}. \quad (2)$$

An observation can be made that the first mode of a vibrating free-free beam has nodal lines identical to the (2,0) mode of a rectangular plate, as shown in Figure 4. indicating that the mode of vibration is similar in nature.

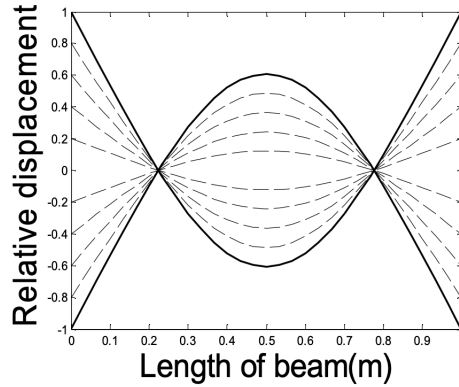


Figure 4: *Mode shape analysis of a free-free beam. Nodal lines are present at approximately 20% of the length from either end of the beam. Figure taken without permission from [7].*

In this paper, this comparison was used to approximate the Young's modulus of elasticity of the rectangular wood plate sampled using resonant frequencies of the (2,0) mode with equation (1), with $n=1$.

The quality factor Q of the resonance can be determined with:

$$Q = \frac{f_0}{\Delta f} \quad (3)$$

Where f_0 is the resonant frequency, and Δf is the bandwidth of the peak 3dB below the maximum.

The internal friction $\tan(\delta)$ of wood can be calculated with the equation:

$$\tan \delta = \tan\left(\pi\sqrt{3}\frac{f_0}{\Delta f}\right) \quad (4)$$

Which can be combined with equation (3) to be written as:

$$\tan \delta = \tan(\pi\sqrt{3}Q^{-1}) \quad (5)$$

The specific gravity γ of an object is defined to be its density divided by the density of the water, where $p_{water} = 997kg/m^3$:

$$\gamma = \frac{p_{wood}}{p_{water}} = \frac{p_{wood}}{997kg/m^3} \quad (6)$$

Equations (1), (5), and (6) can be combined to obtain a ratio known as acoustic conversion efficiency. Different sources in the literature use slight variations of the derivation of this quantity. In this study, the formula by Hamdam et al. [5] was used:

$$ACE = \frac{\sqrt{E_d/\gamma}}{\gamma \tan \delta} \quad (7)$$

Higher values of ACE correspond to a better efficiency at converting vibrations into sound. Larger values of Young's modulus, smaller values for specific gravity, and smaller values of internal friction correspond to greater ACE [5].

3.2 Modelling resonant frequencies

Unfortunately, no analytical solution to the differential equation that governs plate oscillation for rectangular plates with free-free boundary conditions can be derived. However, solutions can be found in the limit of certain plate geometries; namely, square plates and bars. The relations used in this paper are those discussed in *Principles of Vibration and Sound* [4].

The resonant frequency of the (1,1) mode of a square plate is given by:

$$f_{1,1(square)} \approx \frac{h\sqrt{c_x c_y}}{L_y L_x} \sqrt{\frac{1 - \sqrt{v_{xy} v_{yx}}}{2}}. \quad (8)$$

And the frequency of the n th mode of a free-free vibrating bar is given by:

$$f_{n(bar)} = \frac{0.113h}{L_x^2} \sqrt{c_x c_y} [(3.0112)^2, 5^2, \dots, (2n+1)^2]. \quad (9)$$

Where c_x and c_y are defined as:

$$c_x = \sqrt{\frac{E_x}{p(1 - v_{xy} v_{yx})}} \quad (10)$$

$$c_y = \sqrt{\frac{E_y}{p(1 - v_{xy}v_{yx})}} \quad (11)$$

Where L_x is the length of the bar, L_y is the width, h is the thickness, E_x and E_y are the Elastic moduli in the longitudinal and radial directions, and $v_{xy}v_{yx}$ is the product of the longitudinal-radial and radial-longitudinal Poisson's ratios of stress and strain.

The resonant frequencies of the other modes of vibration of square plates can be determined by multiplying Equation (8) by given ratios. For the (2,0) mode of vibration, the ratio is 1.94, giving us:

$$f_{2,0(square)} = 1.94 * f_{1,1(square)} \approx 1.94 \frac{h\sqrt{c_x c_y}}{L_y L_x} \sqrt{\frac{1 - \sqrt{v_{xy}v_{yx}}}{2}}. \quad (12)$$

Numerical values for E_x, E_y, v_{xy} , and v_{yx} were obtained from the Wood Handbook [8]. We used the values for Young's modulus of wood of 12% moisture content, as this provided the closest moisture content to our samples.

As the rectangular plates used in this study were geometrically a combination of a beam and a square plate, it is therefore expected that a combination of the models would be the most effective. Therefore, in this study it is proposed that the resonant frequency of a plate can be approximated via an average of the two pre-existing models, which will be henceforth called the averaged prism model:

$$f_{2,0(prism)} = \frac{f_{1(bar)} + f_{2,0(square)}}{2}. \quad (13)$$

Although errors in measurements of mass and dimensions are present in the approximations given by Equations (8), (9), (11) and (12), such errors are many orders of magnitude below the possible variations in the elasticity moduli of the wood pieces. Hence, such errors are considered negligible. The literature values of elasticity moduli given in the Wood Handbook [8] that are used in the approximations are stated to have a 22% coefficient of variation (standard deviation divided by the mean). Thus, standard deviation of the approximated frequencies have been assumed to arise solely out of this variation in elastic moduli (where one σ is 22% times the mean elastic moduli), and smaller measurement errors have been discarded with regards to the frequency model.

4 Discussion of results

4.1 Frequency and frequency modelling

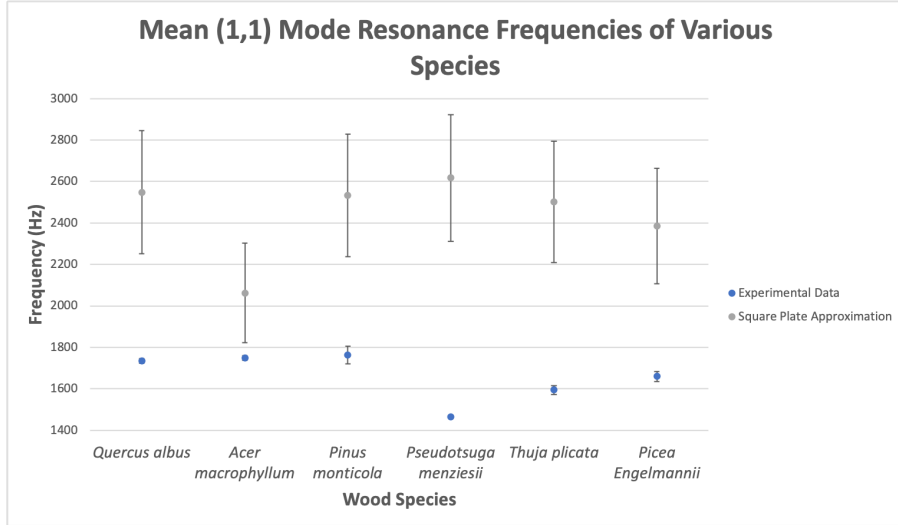


Figure 5: Average resonant frequencies of the (1,1) mode of varying wood species in comparison to the square plate approximation values. Experimental data frequencies were averaged from $N=10$ pieces per species, excepting *Thuja plicata*, which was averaged from $N=6$ pieces. Error bars on experimental data represent standard error of the mean. The square plate approximation values were calculated using values of elastic modulus and Poisson's ratios given in the Wood Handbook [8], experimentally measured values for dimensions and mass, and equation (8). Error bars on the approximation represent upper and lower bounds of approximated frequency, which were derived by reapplying equation (8) to the mean literature Young's modulus value plus or minus one σ .

Analysis of the (1,1) torsional mode of vibration provided no clear relationship between frequency and any other measured values such as density. A notable observation is that the error of the mean of *Pseudotsuga menziesii* is much smaller in comparison to that of other species, indicating the consistency of grain results in a much narrower distribution of resonant frequency values in a given set of wood pieces.

When compared with the experimental data, the (1,1) resonant frequency values given by the square plate approximation consistently overestimate the frequency, with no overlap of error bars. Different wood species have different degrees of overestimation.

When considering the $(2,0)$ mode of vibration, two approximations can be applied - the second mode of vibration of a square plate, and the first mode of vibration of a bar. The nodal lines of both of these are similar to those in a rectangular plate vibrating in the $(2,0)$ mode, as seen in Figure 6 although in rectangular wooden plates the nodal lines are curved whereas in square plates and bars the nodal lines are straight.

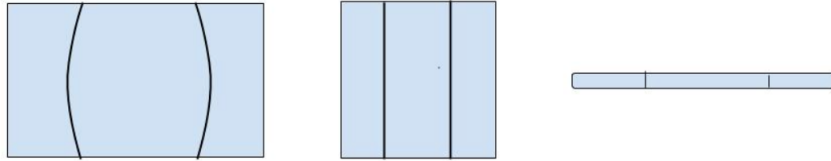


Figure 6: *Visual comparison of $(2,0)$ vibrational bar of rectangular plate (left) and square plate (center) with first mode of vibration of a bar (right).*

When the resonant frequency is calculated, the square plate approximation consistently overestimates whereas the bar equation consistently underestimates. The proposed averaged prism model utilizes this to predict the value of the experimental data well. It should be noted that this averaged prism model can only be applied to vibrational mode of plates of $(n,0)$, where $n > 2$ $n \in \mathbb{N}$. Only for modes of vibration of the plates where the modes are similar with modes of vibrating bars would this model be able to be hypothetically applied. Any modes of vibration (n,m) of the plate where $m > 0$ $m \in \mathbb{N}$ would not have a corresponding vibrational mode in a beam, and thus the model is limited to a subset of plate vibrational modes.

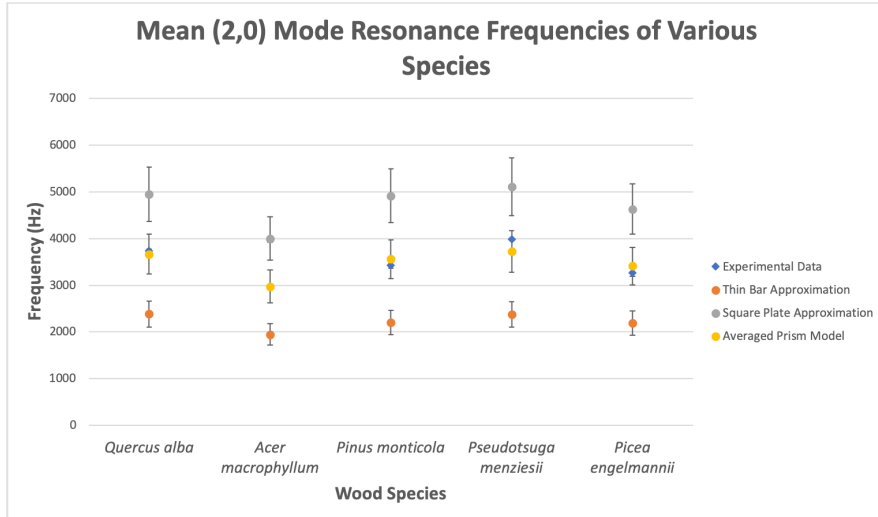


Figure 7: Average Resonant Frequencies of the (2,0) Mode of varying wood species in comparison to the square plate, thin beam, and averaged prism approximation values. Experimental frequencies were averaged from $N=8$ pieces for *Pinus monticola*, $N=9$ pieces for *Picea engelmannii*, and $N=10$ pieces for all other species. Error bars on experimental data represent standard error of the mean. The approximation values were calculated using values of Elastic modulus and Poisson’s ratios given in the Wood Handbook [8], experimentally measured values for dimensions and mass, and equations (8), (9), and (10). Error bars on the approximation represent upper and lower bounds of approximated frequency, which were derived by reapplying equations (8), (9), and (10) to the mean literature Young’s modulus value plus or minus one σ .

The averaged prism model was found to be an accurate model for four of the five species tested. For *Quercus alba*, *Pinus monticola*, *Pseudotsuga menziesii*, and *Picea engelmannii* the experimental resonant frequency falls within the error bars of the model. There is a significant degree of variation within the Young’s Modulus in a species, and thus the model can be considered a sufficient approximation for the species so long as the experimental values falls within one standard deviation of the model.

The sole species for which the averaged prism model was not effective was *Acer macrophyllum*, whose data is approximated best by the square plate approximation. A discussion of this discrepancy will be provided later in the paper.

Overall, the averaged prism model was found to be most accurate. This aligns with the geometry of our rectangular plates, which are geometrically in-between squares and bars. It can be hypothesized that for plates of other dimensions a weighted mean of the two approximations could be used, though the investigation of this lies beyond the scope of this study.

4.2 Young’s modulus and acoustic conversion efficiency

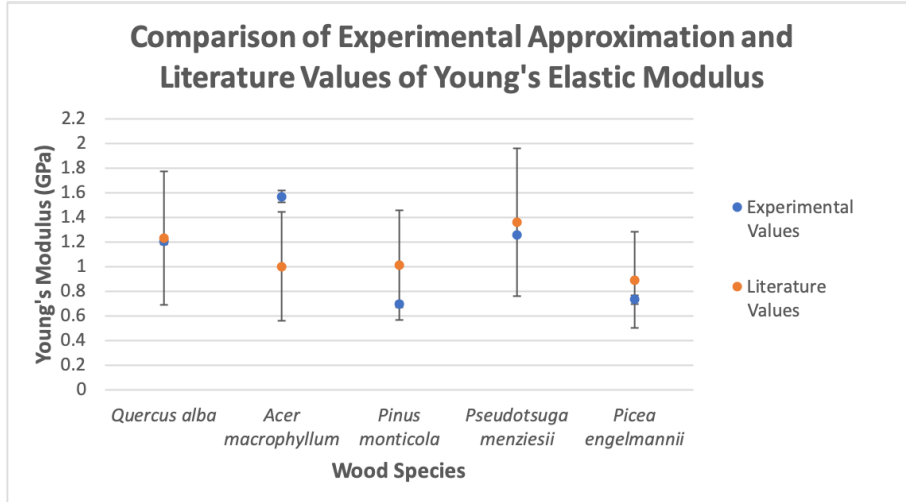


Figure 8: *Computed Young’s Moduli of various wood species. The calculated values are the mean of each sample ($N=8$ for *Pinus monticola*, $N=9$ for *Picea engelmannii*, and $N=10$ for all other species), where the Young’s modulus of each piece was approximated using Equation (1). Error bars on calculated values represent standard error of the mean. Calculated values are compared with the literature values of 12% MC wood in the Wood Handbook [8]. Error bars on the Literature Values represent 2 standard deviations based off the 22% coefficient of variation.*

When looking at the experimental Young’s Modulus values, the beam approximation (1) gives values of elasticity modulus that generally agree with the Wood Handbook [8]. Mean elastic modulus for the samples of *Quercus Alba*, *Pseudotsuga menziesii*, and *Picea engelmannii* fall within one σ of the mean literature value, and mean elastic modulus of the samples of *Pinus monticola* fall within two σ of the literature value. Interestingly, much like with the averaged prism model, the exception is *Acer macrophyllum*, for which the mean elastic modulus of the samples does not fall within two σ of the literature value.

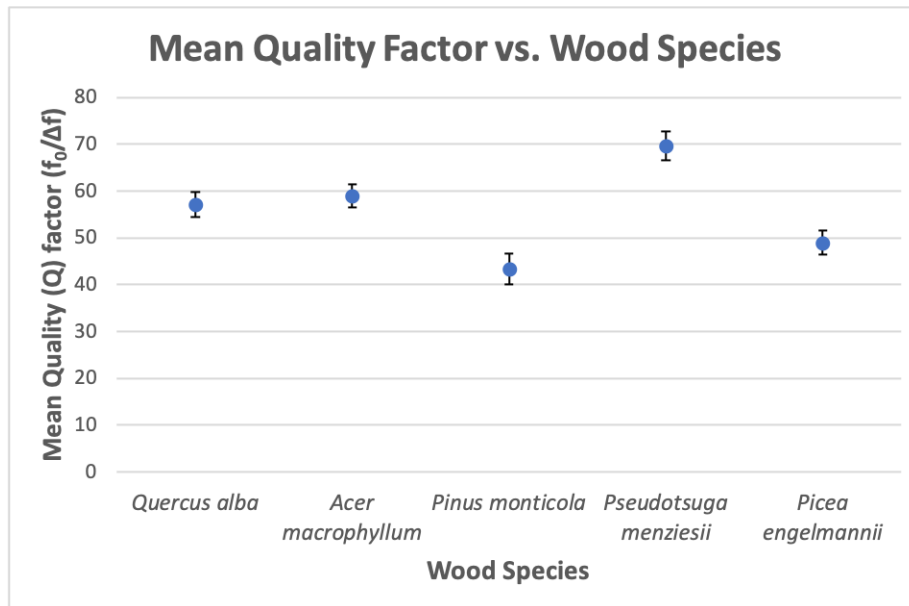


Figure 9: Mean Quality factor of various species of wood. The Quality Factor of each sample was calculated using Equation (3), and the mean of each species was then taken ($N=8$ for *Pinus monticola*, $N=9$ for *Picea engelmannii*, and $N=10$ for all other species). The error bars represent standard error of the mean.

When comparing the mean quality factors of the tested wood species, all fall into a range of 45 to 70. The mean of *Pseudotsuga heterophylla* is noticeably higher, indicating that it oscillates with the least energy loss. *Pinus monticola* has both the lowest value, as well as the largest standard error.

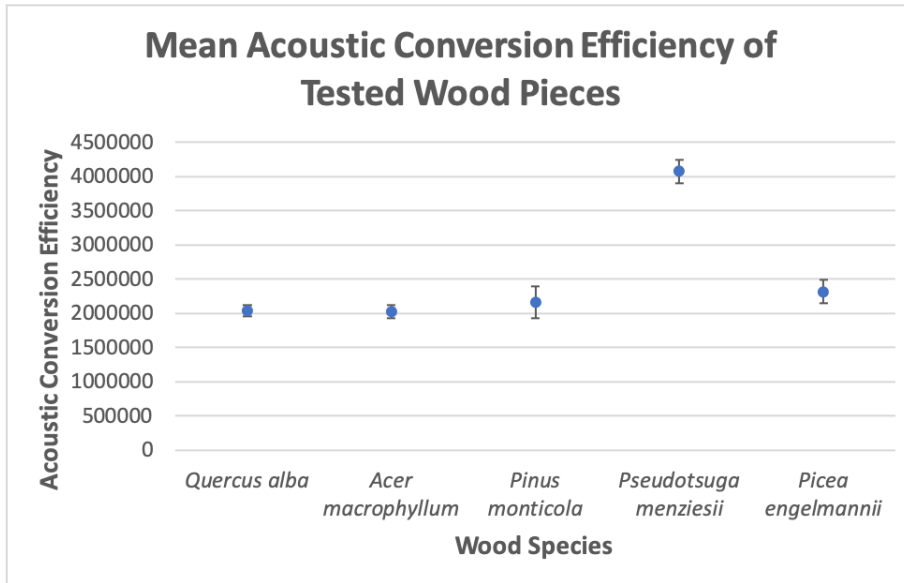


Figure 10: Mean acoustic conversion efficiency factor of various species of wood. The ACE of each sample was calculated using Equation (7), and the mean of each species was then calculated ($N=8$ for *Pinus monticola*, $N=9$ for *Picea engelmannii*, and $N=10$ for all other species). The error bars represent standard error of the mean.

The acoustic conversion efficiency of the tested species was overall similar, with the exception of the noticeably higher *Pseudotsuga menziesii*. A one-way ANOVA statistical test yielded a $p < 0.000001$, suggesting one (or more) treatments was statistically significantly different. A post-hoc Tukey's HSD test yielded $p < 0.01$ for comparisons of *Pseudotsuga menziesii* with all other varieties, and $p > 0.01$ (ranging from 0.64 to 0.89) for all other comparisons, indicating that there is a statistically significant difference between *Pseudotsuga menziesii* and other varieties, but not between other varieties.

A relationship of interest is the correlation between consistent wood grain and high acoustic conversion efficiency. Although it is possible that *Pseudotsuga menziesii* has a higher acoustic conversion efficiency relative to the tested wood types, another possible explanation of the results is that wood plates with consistent grain have higher efficiency compared to plates that have inconsistent grain or imperfections in the grain.

5 Discussion of errors

The most apparent error, both in the approximation of Young’s modulus of Elasticity and in the model for approximating the (2,0) mode resonant frequency was the discrepancies with regard to *Acer macrophyllum*. A comparison of specific gravity measured from the samples (using equation (6)) with those found for the species in the Wood Handbook shows a possible reason for the discrepancy:

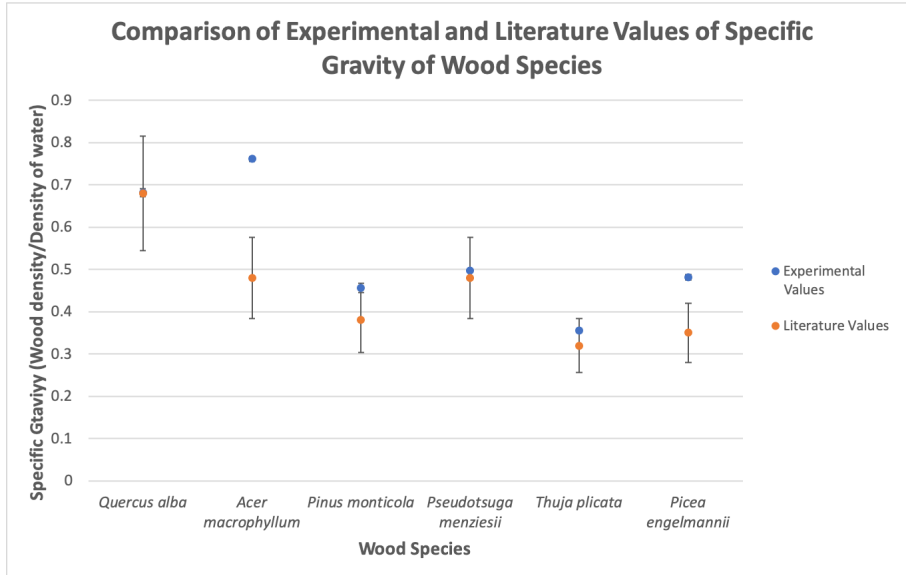


Figure 11: *Experimental and literature values of specific gravity of the tested wood species. Experimental values are in blue, and represent the mean specific gravity of the ten samples. Error bars on experimental values represent standard error of the mean. Orange dots represent the specific gravity values for 12% moisture content wood given in the Wood Handbook [8]. Error bars on the literature values represent two standard deviations, calculated from the 10% coefficient of variation of specific gravity.*

The above results show that the specific gravity values of the samples of *Quercus alba*, *Pinus monticola*, *Pseudotsuga menziesii*, and *Thuja plicata* are in agreement with the literature values. It is noticeable that the specific gravity value for *Picea engelmannii* is greater than the mean literature value by approximately 0.13, and the value for *Acer macrophyllum* is greater than the literature value by approximately 0.28. This would imply that the density of the experimental samples of these two wood species is greater than that of the density of literature values, especially with regards to *A. macrophyllum*.

In consideration of the dependence of Young’s modulus and frequency on density and specific gravity (with regard to equations (1), (9), (11), and (12))

it is entirely possible that this difference from literature and experimentally measured density of *A. macrophyllum* leads to the discrepancy. A significantly higher density would result in Young's modulus and frequency values that are higher than those the literature values used. This larger density value could be explained by the samples being drier than the literature moisture content of 12%, or on misidentification of the wood species, though the latter case is quite unlikely.

Being unable to measure the exact moisture content of the samples, another source of error arises from comparing the experimental values to literature values for 12% moisture content wood. The samples used had a possible range of moisture content from 6-12% depending on the extent of kiln drying. This could possibly have an affect on the ability to accurately compare literature and experimental values.

Measurement errors in weighing, measuring dimensions, and measuring resonant frequencies were also present to a degree. These were minimized by repeating measurements multiple times.

Other experimental errors arise from assumptions made in applying mathematical equations. Equation (1) normally is applied to wooden beams, and although its application returns elasticity moduli that agree with the literature value, there are factors of plate vibration that are unaccounted for. Thus the equation can give an estimate but not an exact value. Equations (9) and (10) also assume objects of a beam-like or square like nature, and perfectly consistent wood grain. Imperfections in the wood are not accounted for and thus error could have been produced to varying degrees depending on the sample. The variance in wood grain consistency between the different specimens is also an experimental error. It is an uncontrolled factor between the species, and due to this factor, it cannot be definitely concluded whether trends in the data are due to material differences in species or differences in wood grain consistency. However, correlations can still be observed.

6 Conclusion

When predicting resonant frequency values for modes higher than $(n,0)$ (where $n > 2$ $n \in \mathbb{N}$) in a free-free rectangular wooden plate, an average of the bar and square plate approximations was most accurate in predicting experimental values. Although more complex numerical approximations for frequencies of plate vibrations exist, for this subset of vibrational modes this derived simple approximation provided a very good estimate for the dimensions of plates studied.

Out of tested species, *Pseudotsuga menziesii* had the highest mean ACE value, near double of all of the others, and thus is the most efficient at converting energy into sound. This would indicate that out of the tested specimens, the *P. menziesii* boards were the best suited for usage as soundboards in musical instruments. However, it is unclear whether the higher relative ACE value of *P. menziesii* is a result of the characteristics of it as a species, or simply a consequence of its more consistent wood grain relative to the rest of the specimens. One possible interpretation of the data is that it provides numerical support for the inviability of inconsistent-grain wood for usage in musical instruments, as all specimens with inconsistent wood grain demonstrated lower values of ACE.

7 Acknowledgements

We would like to thank Dr. Robert Raussendorf for being our informative mentor, Dr. Chris Waltham for his expert advice on the physics of sound and the mechanisms of acoustical measurements, and Dr. James Charbonneau for the initial idea of the project and for the love of physics that he has inspired.

8 Appendix - Supplemental graphs

Graphs of the data and model values of the (2,0) resonant frequencies of individual pieces are given below.

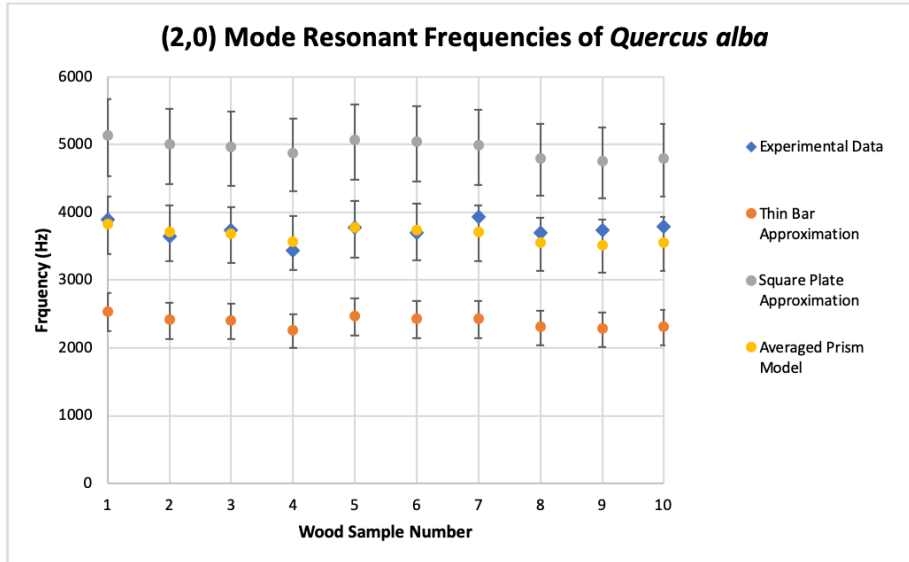


Figure 12: Resonant Frequencies of the (2,0) mode of *Quercus alba*. Mean resonant frequency was determined by averaging frequency values from 20 taps. Experimental data is plotted as diamonds, and model values are plotted as circles. Error bars on the data represent standard error of the mean, but are too small to be visible (Error < 10 Hz). Approximations were calculated using values of Elastic modulus and Poisson's ratios given in the Wood Handbook [8], experimentally measured values for dimensions and mass, and equations (9) and (11). Error bars on the approximation represent upper and lower bounds of approximated frequency, which were derived by reapplying equation (8) to the mean literature Young's modulus value plus or minus one standard deviation. Averaged prism model values were determined by averaging the two approximations.

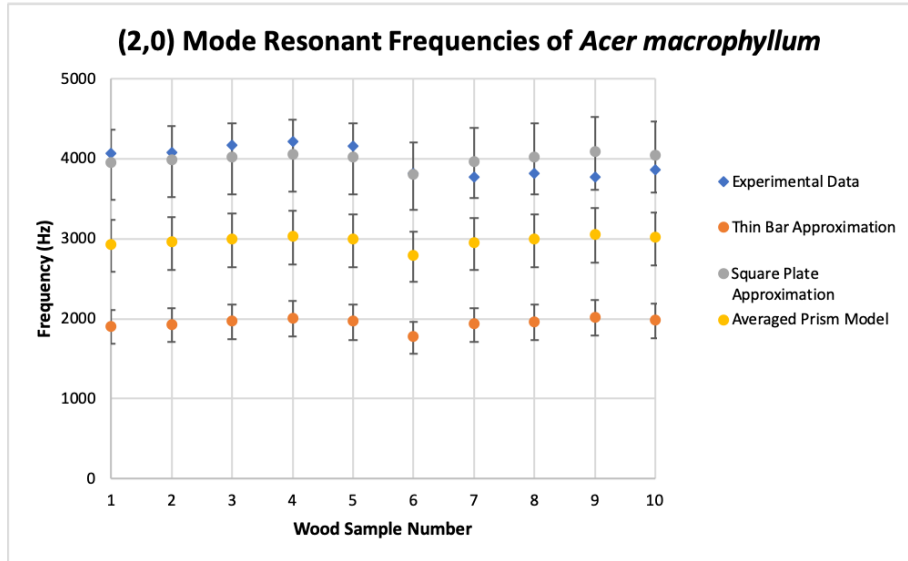


Figure 13: Resonant Frequencies of the $(2,0)$ mode of *Acer macrophyllum*. Mean resonant frequency was determined by averaging frequency values from 20 taps. Experimental data is plotted as diamonds, and model values are plotted as circles. Error bars on the data represent standard error of the mean, but are too small to be visible (Error < 10 Hz). Approximations were calculated using values of Elastic modulus and Poisson's ratios given in the Wood Handbook [8], experimentally measured values for dimensions and mass, and equations (9) and (11). Error bars on the approximation represent upper and lower bounds of approximated frequency, which were derived by reapplying equation (8) to the mean literature Young's modulus value plus or minus one standard deviation. Averaged prism model values were determined by averaging the two approximations.

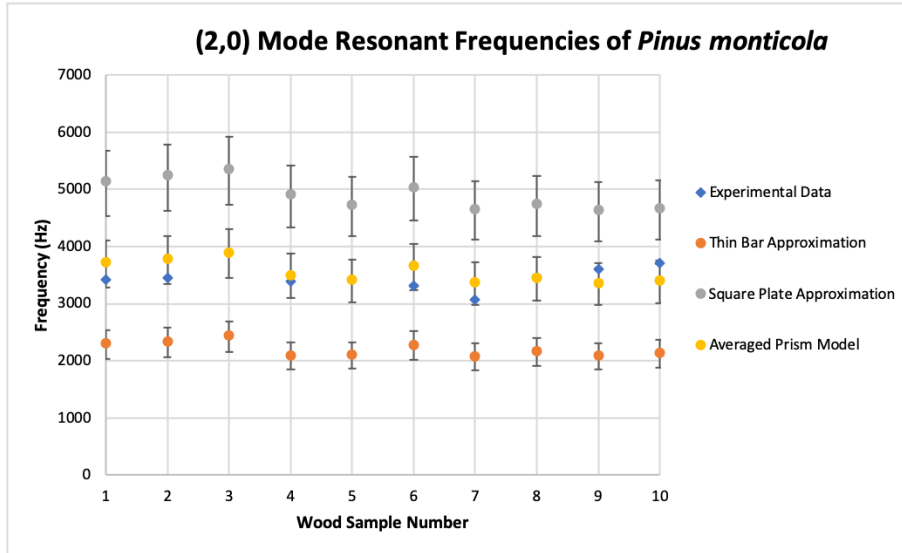


Figure 14: Resonant Frequencies of the $(2,0)$ mode of *Pinus monticola*. Mean resonant frequency was determined by averaging frequency values from 20 taps. Experimental data is plotted as diamonds, and model values are plotted as circles. Error bars on the data represent standard error of the mean, but are too small to be visible (Error < 10 Hz). Approximations were calculated using values of Elastic modulus and Poisson's ratios given in the Wood Handbook [8], experimentally measured values for dimensions and mass, and equations (9) and (11). Error bars on the approximation represent upper and lower bounds of approximated frequency, which were derived by reapplying equation (8) to the mean literature Young's modulus value plus or minus one standard deviation. Averaged prism model values were determined by averaging the two approximations.

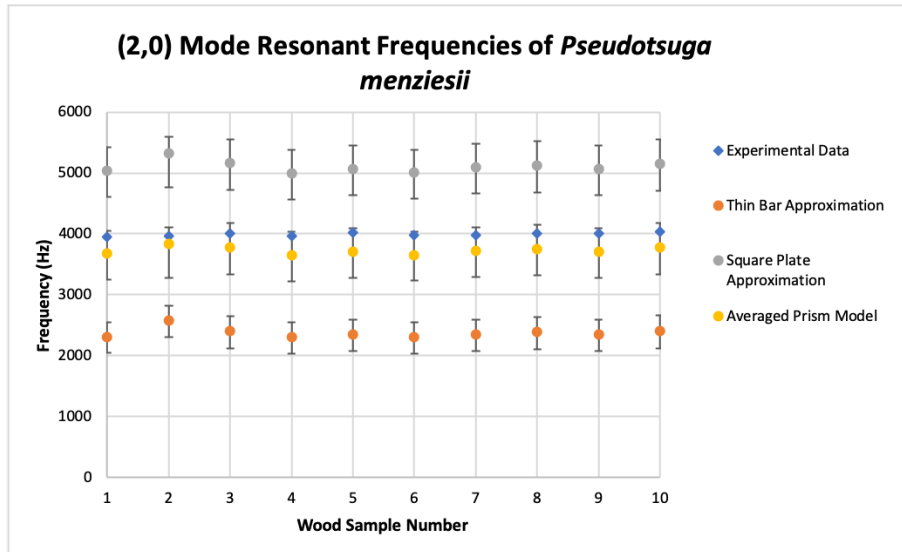


Figure 15: Resonant Frequencies of the $(2,0)$ mode of *Pseudotsuga menziesii*. Mean resonant frequency was determined by averaging frequency values from 20 taps. Experimental data is plotted as diamonds, and model values are plotted as circles. Error bars on the data represent standard error of the mean, but are too small to be visible (Error < 10 Hz). Approximations were calculated using values of Elastic modulus and Poisson's ratios given in the Wood Handbook [8], experimentally measured values for dimensions and mass, and equations (9) and (11). Error bars on the approximation represent upper and lower bounds of approximated frequency, which were derived by reapplying equation (8) to the mean literature Young's modulus value plus or minus one standard deviation. Averaged prism model values were determined by averaging the two approximations.

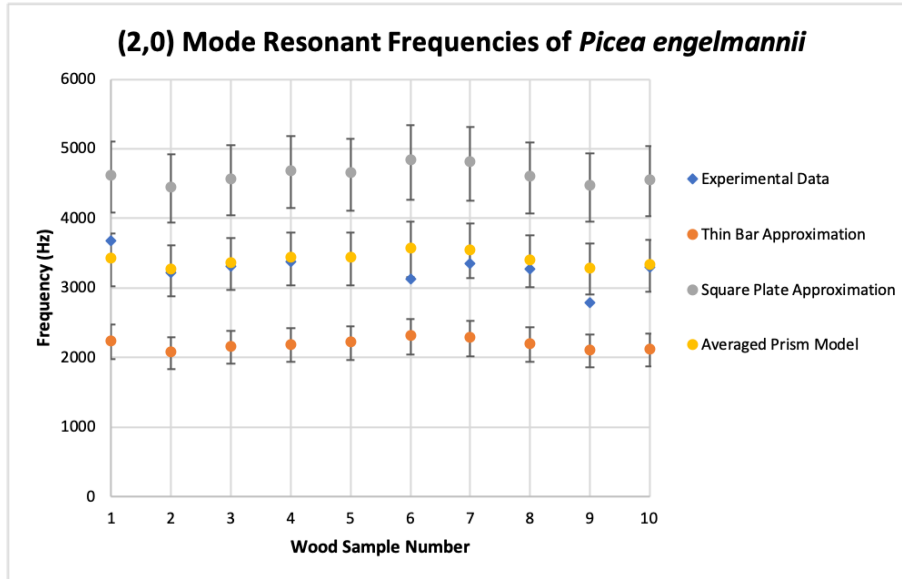


Figure 16: *Resonant Frequencies of the (2,0) mode of Picea engelmannii.* Mean resonant frequency was determined by averaging frequency values from 20 taps. Experimental data is plotted as diamonds, and model values are plotted as circles. Error bars on the data represent standard error of the mean, but are too small to be visible ($\text{Error} < 10 \text{ Hz}$). Approximations were calculated using values of Elastic modulus and Poisson's ratios given in the Wood Handbook [8], experimentally measured values for dimensions and mass, and equations (9) and (11). Error bars on the approximation represent upper and lower bounds of approximated frequency, which were derived by reapplying equation (8) to the mean literature Young's modulus value plus or minus one standard deviation. Averaged prism model values were determined by averaging the two approximations.

9 References

- [1] Ono T. and Norimoto, M. On physical criteria for the selection of wood for soundboards of musical instruments. *Rheol Acta* **23**, 652-656 (1984).
- [2] Barnett, R. and Bonham, V. Cellulose microfibril angle in the cell wall of wood fibres. *Biol Rev Camb Philos Soc.* **79**, 461-472 (2004).
- [3] Hearmon, R. The fundamental frequency of vibration of rectangular wood and plywood plates. *Proc. Phys. Soc.* **58**, 78-92 (1945).
- [4] Rossing D. and Fletcher N. Principles of Vibration and Sound. *Springer Science+Business Media, LLC.* (2004).
- [5] Hamdaan, S., Josuh I., Rahman, M. and Juan, M. Acoustic properties of *Syzygium* sp., *Dialium* sp., *Gymnostoma* sp., and *Sindora* sp. wood. *BioResources* **11**, 5941-5948 (2016).
- [6] Pintelon, R., Guillame, P., De Belder, K., and Rolain, Y. Measurement of Young's modulus via modal analysis experiments: A system identification approach. *IFAC Proceedings Volumes* **36**, 375-380 (2003).
- [7] Parijat, A., Sehgal, S., Singh, T. and Kumar, H. Mode shape analysis of free-free beam. *Proc. of Int conf. On Emerging Trends in Engineering and Technology* (2016).
- [8] Green, D., Winandy, J. and Kretschmann, D. Wood Handbook - Wood as an engineering material. *US Dept. of Agriculture, Forest Service, Forest Products Laboratory* (1999).